Charge Screening by Internal pH and Polyvalent Cations as a Mechanism for Activation, Inhibition, and Rundown of TRPM7/MIC Channels

J. Ashot Kozak,[1] Masayuki Matsushita,[2] Angus C. Nairn,[3] and Michael D. Cahalan[1]

[1]Department of Physiology and Biophysics, School of Medicine, University of California, Irvine, CA 92697
[2]First Department of Physiology, Okayama University Medical School, 2-5-1 Shikata-cho, Okayama 700-8558, Japan
[3]Department of Psychiatry, Yale University School of Medicine, New Haven, CT 06508

The Mg^{2+}-inhibited cation (MIC) current, believed to represent activity of TRPM7 channels, is found in lymphocytes and mast cells, cardiac and smooth muscle, and several other eukaryotic cell types. MIC current is activated during whole-cell dialysis with divalent-free internal solutions. Millimolar concentrations of intracellular Mg^{2+} (or other divalent metal cations) inhibit the channels in a voltage-independent manner. The nature of divalent inhibition and the mechanism of channel activation in an intact cell remain unknown. We show that the polyamines (spermine, spermidine, and putrescine) inhibit the MIC current, also in a voltage-independent manner, with a potency that parallels the number of charges. Neomycin and poly-lysine also potently inhibited MIC current in the absence of Mg^{2+}. These same positively charged ions inhibited IRK1 current in parallel with MIC current, suggesting that they probably act by screening the head group phosphates on PIP_2 and other membrane phospholipids. In agreement with this hypothesis, internal protons also inhibited MIC current. By contrast, tetramethylammonium, tetraethylammonium, and hexamethonium produced voltage-dependent block but no inhibition. We show that inhibition by internal polyvalent cations can be relieved by alkalinizing the cytosol using externally applied ammonium or by increasing pH in inside-out patches. Furthermore, in perforated-patch and cell-attached recordings, when intracellular Mg^{2+} is not depleted, endogenous MIC or recombinant TRPM7 currents are activated by cytosolic alkalinization and inhibited by acidification; and they can be reactivated by PIP_2 following rundown in inside-out patches. We propose that MIC (TRPM7) channels are regulated by a charge screening mechanism and may function as sensors of intracellular pH.

INTRODUCTION

To date, 30 or so members of the mammalian TRP superfamily have been identified and subdivided into smaller groups based on sequence comparison: these include TRPC, TRPM (melastatin), and TRPV channels. The majority of expressed TRP proteins are nonselective cation channels, but some, such as TRPV5 and TRPV6, are highly Ca^{2+} selective. For a number of these channels the modes of activation have been elucidated. For example, TRPV1 is activated by heat and vanilloid compounds; TRPM8 by cold and menthol; TRPM2 is activated in response to intracellular ADP ribose; and TRPM4 and TRPM5 are activated by elevation of cytosolic Ca^{2+}. Thus, in many cases, TRP channels appear to function as cellular detectors of various biochemical and sensory stimuli (Minke and Cook, 2002; Montell et al., 2002; Clapham, 2003). TRPM7 is unusual in that it has a functional eEF2-like kinase domain at its COOH terminus and belongs to the three-member "chanzyme" group of TRPMs, which includes TRPM6, a close homologue, and TRPM2, an ADP-ribose pyrophosphatase (for review see Montell et al., 2002). The hallmark of TRPM7 channel activity is its inhibition by millimolar

levels of intracellular Mg^{2+} (Nadler et al., 2001). Nadler et al. suggested that Mg^{2+}-ATP might be responsible for inhibition (see also Prakriya and Lewis, 2002). However, we subsequently showed that free Mg^{2+}, rather than Mg^{2+}-ATP, is the active species (Kozak and Cahalan, 2003). Consequently, we accept the nomenclature for the native channel as MIC, for Mg^{2+}-inhibited cation current (Kozak et al., 2002; Prakriya and Lewis, 2002; for review see Clapham, 2002).

Upon establishment of the whole-cell recording configuration, the normally absent MIC current (I_{MIC}) develops gradually over the course of minutes when the pipette solution lacks Mg^{2+}. Even though intracellular free Mg^{2+} levels in mammalian cells are thought to be 500 μM–1 mM (Ng et al., 1991; Grubbs, 2002), usually 3–4 mM free Mg^{2+} is necessary to inhibit I_{MIC} completely; and the same is true for heterologously expressed TRPM7 current (Nadler et al., 2001; Kozak et al., 2002; Prakriya and Lewis, 2002). Thus, tonic inhibition by Mg^{2+} cannot fully explain why MIC current is not active in intact cells or in the perforated-patch configuration

---

Correspondence to Michael D. Cahalan: mcahalan@uci.edu

Abbreviations used in this paper: CHO, Chinese hamster ovary; MBP, myelin basic protein; MIC, Mg^{2+}-inhibited cation.

(Kozak et al., 2002; Jiang et al., 2003). Conversely, it appears unlikely that slow development of I_{MIC} during whole-cell recording simply reflects gradual disinhibition by Mg^{2+}. To date, the mechanism of MIC current activation under physiological conditions (without cell dialysis) remains enigmatic. It was proposed that TRPM7 channels mediate intracellular Mg^{2+} homeostasis by serving as a Mg^{2+} influx pathway when internal $[Mg^{2+}]$ falls (Schmitz et al., 2003; for review see Montell, 2003). It remains unexplained, however, under what circumstances the Mg^{2+} content of a cell would fall so dramatically as to activate substantial I_{MIC}.

We showed previously that in addition to Mg^{2+}, other divalent metal cations such as Mn^{2+}, Ba^{2+}, Sr^{2+}, and Zn^{2+} at similar concentrations also inhibit I_{MIC} from the inside (Kozak and Cahalan, 2003). As is the case with internal Mg^{2+}, the inhibition by other divalent cations is voltage independent, occurs more slowly than expected for diffusion into the cytosol, and is therefore unlikely to reflect direct ion channel pore block. Two recent studies show that in addition to inhibiting channel activity, cytosolic Mg^{2+} affects the intrinsic kinase of TRPM7. Increasing the Mg^{2+} concentration from micromolar to millimolar levels substantially increased phosphotransferase activity measured in vitro (Schmitz et al., 2003; Ryazanova et al., 2004). It was suggested, therefore, that the Mg^{2+}-binding site responsible for current reduction may be the ATP-binding pocket of the kinase domain (Schmitz et al., 2003; for review see Montell, 2003). Ryazanova et al. (2004) subsequently demonstrated that other divalent metals have distinct effects on the kinase activity of TRPM7: Mn^{2+} is stimulatory, Zn^{2+} is inhibitory, and Ca^{2+} is without effect. Recently we showed that both Zn^{2+} and Ca^{2+} inhibit heterologously expressed TRPM7 channel activity, similar to Mg^{2+}, indicating that the divalent metal effects on the kinase and the channel proceed by a different mechanism. Moreover, a "kinase-dead" point mutant showed no difference in expression, activation, or Mg^{2+} inhibition, compared with wild-type TRPM7 channel activity (Matsushita et al., 2005). These results indicate that the kinase and channel activities are separable.

In this study we test a different hypothesis for internal Mg^{2+} inhibition of the channel: negatively charged membrane phospholipids are considered as the target for modulating channel activity. It was previously shown that TRPM7 current amplitude was diminished due to reduction in $PI(4,5)P_2$ levels (Runnels et al., 2002). In agreement with this finding we showed that the rundown of I_{MIC} proceeds roughly in parallel with the endogenous IRK1 channel current in RBL cells, suggesting that the same process, depletion of membrane $PI(4,5)P_2$, is the cause of rundown in both channels (Kozak et al., 2002). Here, we test other positively charged ions such as polyamines and protons for their inhibitory effects and identify them as potential physiological inhibitors of MIC/TRPM7 currents. Interestingly, we find that during perforated-patch recording, which prevents cytosolic Mg^{2+} depletion, and in cell-attached and inside-out patches, intracellular alkalinization activates the current. In inside-out patches, effects of PIP_2 and acid pH oppose each other. Furthermore, constitutively active TRPM7 channel activity is reversibly inhibited in the cell-attached mode when the intact cell interior is acidified. Thus, we demonstrate that TRPM7 can serve as an intracellular pH sensor. We also show that the TRPM7 phosphotransferase activity is modulated by pH in vitro. The channel and kinase domains exhibit different pH sensitivities, further indicating the independence of their activities (Matsushita et al., 2005). Preliminary reports of these results have appeared (Kozak and Cahalan, 2004; Kozak et al., 2005).

MATERIALS AND METHODS

Cells
RBL-2H3 cells (Siraganian et al., 1982) were grown in EMEM (Cambrex) supplemented with 10% FBS. Chinese Hamster Ovary (CHO-K1) cells were grown in F-12K medium (American Type Culture Collection) and 10% FBS. The cell lines were passaged every 2 d. Human (resting) peripheral T lymphocytes were isolated from blood using the Rosette Sep enrichment kit (StemCell Technologies) and maintained in RPMI 1640 medium with added 1 mM L-glutamine and 10% FBS. Recordings were made 1–6 d after T cell isolation. Cells were kept in a 5% CO_2 cell culture incubator at 37°C.

Expression of TRPM7 in CHO-K1 Cells
CHO cells were grown on six-well polystyrene plates and transiently transfected with the mouse TRPM7 wild-type or TAP mutant clones in the pcDNA3.1 vector (Invitrogen) using the Effectene transfection kit (QIAGEN) according to the manufacturer's instructions and as previously described (Matsushita et al., 2005). Cells were cotransfected with the eGFP plasmid (CLONTECH Laboratories, Inc.) for visualization (Chalfie et al., 1994). Transfectant was kept on cells for at least 12 h for efficient gene expression. The cells were replated on acid-washed glass coverslip chambers ~24 h before electrophysiological recordings. The chambers were mounted on the stage of an inverted Carl Zeiss IM35 microscope equipped with a mercury lamp light source to visualize GFP fluorescence. Recordings were performed 3–4 d after transfection.

Patch Clamp Recording
Macroscopic and single channel currents were recorded in the whole-cell, cell-attached, and inside-out patch recording configurations using a computer-operated EPC-9 patch clamp amplifier (HEKA Elektronik). Electrophysiological data acquisition and initial processing were done using Pulse/Pulsefit (HEKA) software. Igor Pro (WaveMetrics) and Microcal Origin (Microcal Software) were used for further analysis. Patch pipettes were pulled using a programmable puller (Zeitz Instruments) from borosilicate glass capillaries (Garner Glass Company). Pipettes were coated with Sylgard (Dow Corning Corp.) close to the tips and fire-polished on a microforge (Narishige) to a resistance of

2–4 MΩ when filled with internal solutions. For obtaining patches on CHO-K1 cells we used pipettes with resistances ∼1 MΩ. Currents were sampled at 5–25 kHz and digitally filtered off-line at 1 kHz. The membrane potential was held at 0 or −10 mV, and currents were monitored during voltage ramps from −110 mV to +85 mV or voltage steps. Voltage ramp or step stimuli were delivered at 0.5 Hz. Slow and fast capacitative transients were canceled by the compensation circuitry of the EPC-9. Cells were superfused with various solutions by bath exchange. Rapid solution exchanges were performed using a SF-77 perfusion system (Warner Instruments Inc., Hamden, CT). All recordings were done at room temperature (∼21°C).

The Ca^{2+}-containing external solution contained (in mM) 2 $CaCl_2$, 167 Na^+ aspartate, 2 Cs^+ methanesulfonate, 10 HEPES, 2 glucose, pH 7.3 titrated with NaOH. The divalent-free external solutions consisted of 144 Cs^+ aspartate, 5 CsCl, 2 Cs^+ methanesulfonate, 10 HEDTA, 10 HEPES, 2 glucose, pH 7.3 titrated with CsOH; or 154 Cs^+ aspartate, 5 CsCl, 2 Cs^+ methanesulfonate, 1 HEDTA, 10 HEPES, 2 glucose, pH 7.3. Monovalent MIC current refers to recordings in divalent-free external solution. The solution for recording IRK1 current contained (in mM) 4.5 KCl, 2 $CaCl_2$, 150 Na^+ aspartate, 10 HEPES, 2 glucose, pH 7.3. In external solutions containing various quantities of formate, acetate, and propionate, an equimolar amount of Na^+ aspartate was replaced with the corresponding Na^+ salt. The standard pipette solution contained 130 Cs^+ glutamate, 8 NaCl, 0.9 $CaCl_2$, 12 EGTA, 10 HEPES, pH 7.3 titrated with CsOH. Where mentioned, $MgCl_2$ was added to this solution for I_{MIC} inhibition. For cell-attached and excised inside-out recording of TRPM7 current, 1 mM HEDTA was added to the pipette solution to eliminate external block by residual divalent metal cations. For monovalent TRPM7 current recording the membrane voltage was stepped to −100 mV for 300–400 ms followed by a ramp to + 85 mV. Maxchelator software was used to estimate the free Mg^{2+} and Ca^{2+} concentrations. Na^+ aspartate was substituted equimolarly with NH_4^+ aspartate where mentioned. The osmolality of the solutions was adjusted to ∼300–310 mOsm/kg with mannitol. Aspartate and glutamate were used as the principal anions to minimize contaminating chloride currents.

Perforated patch recording was performed as previously described (Rae et al., 1991; Kozak et al., 1998). Aliquots of 60 mg/ml amphotericin B (Sigma-Aldrich) stock solution (in DMSO) were stored at −20°C. Before the experiment, an aliquot was thawed and dissolved in the pipette solution yielding a final concentration of 200 µg/ml. The perforated-patch internal solution contained (in mM) 55 CsCl, 65 Cs_2SO_4, 7 $MgCl_2$, 1 $CaCl_2$, 10 HEPES, pH 7.3. These Mg^{2+} and Ca^{2+} amounts would be sufficient to inhibit I_{MIC} completely if the patch were ruptured and whole-cell recording mode established inadvertently.

A $PI(4,5)P_2$ diC8 (Echelon Biosciences) stock was prepared in distilled water, aliquoted in conical glass vials (Fisher Scientific), and stored at −20°C. Poly-L-lysine hydrobromide (molecular weight 500–2000), putrescine, neomycin sulfate and other salts were purchased from Sigma-Aldrich. Spermine and spermidine were from Calbiochem and hexamethonium bromide was from MP Biomedicals.

pH Dependence of TRPM7 Kinase Activity

The GST fusion protein, consisting of residues 1580–1863 of TRPM7 (GST-TRPM7-KD), was expressed in *Escherichia coli* (DE3) and purified using standard methods (Matsushita et al., 2005). Reaction mixtures (100 µl) contained 50 mM HEPES, 10 mM Mg^{2+} acetate, 5 mM dithiothreitol, 100 µM [^{32}P]ATP (specific activity, 2–5 × 10^2 cpm/pmol), and GST-TRPM7-KD (10 µg/ml), with myelin basic protein (MBP, 50 µg/ml) as substrate. For analysis of the effect of pH on the kinase activity, GST-TRPM7-KD was incubated with MBP in reaction mixtures at various pH values. All reactions were initiated by the addition of [^{32}P]ATP and performed at 30°C for 10 min. Gels were subjected to autoradiography and analysis using a PhosphorImager (Fuji).

RESULTS

Inhibition of MIC Current by Internal Cations

Fig. 1 A shows the typical development of MIC current in an RBL cell when internal Mg^{2+} is reduced during whole cell recording and dialysis using a pipette solution that contained EDTA to chelate divalent ions. After an initial delay, I_{MIC} increased slowly and reached a maximum ∼6 min after break-in. The inset shows the current–voltage relation obtained at 10 min. Fig. 1 B illustrates preactivated MIC currents, occasionally present in RBL cells immediately following break-in to achieve whole cell recording. Inclusion of internal La^{3+} (top traces) in the pipette resulted in a gradual reduction of the current, inhibiting it completely after ∼120 s of dialysis. La^{3+} also prevented the slower development of MIC current that would normally occur. In addition to divalent metal cations tested previously (Kozak and Cahalan, 2003), Ca^{2+} also inhibited preactivated MIC current and its development in RBL cells (averaged data summarized in Fig. 1 C), similar to its inhibition of expressed recombinant TRPM7 currents (Matsushita et al., 2005).

To distinguish between a low affinity Mg^{2+}-binding site, as is the case for BK Ca^{2+}-activated K^+ channels (Golowasch et al., 1986; Shi and Cui, 2001), and a less specific charge-screening effect (McLaughlin et al., 1981; McLaughlin, 1989; Langner and Kubica, 1999), we evaluated effects of internal polyamines (spermine, spermidine, and putrescine), organic cations that possess increasing charge with increasing chain length. Spermine (4 mM), with a charge of +4 at pH 7.0, completely inhibited the development of MIC current (Fig. 1 B, bottom). Spermidine with a charge of +3 was less potent than spermine, and putrescine (+2) had no significant effect (Fig. 1 C). We also tested other polyvalent cations that have been used to screen and reverse the negative charge on phosphoinositides and phosphatidylserine. Neomycin is an aminoglycoside antibiotic that binds to PIP_2 (Schacht, 1976; Prentki et al., 1986; Gabev et al., 1989) and inhibits K(ATP) channel activity by screening anionic lipid head groups such as PIP_2 (Fan and Makielski, 1997). Poly-L-lysine also inhibits K(ATP) channels most likely by a similar charge screening mechanism (Shyng and Nichols, 1998). In accordance with the idea of charge screening, poly-L-lysine (heterogenous charge from +3 to +6) and neomycin (+6) potently inhibited MIC current development in RBL cells (Fig. 1 C).
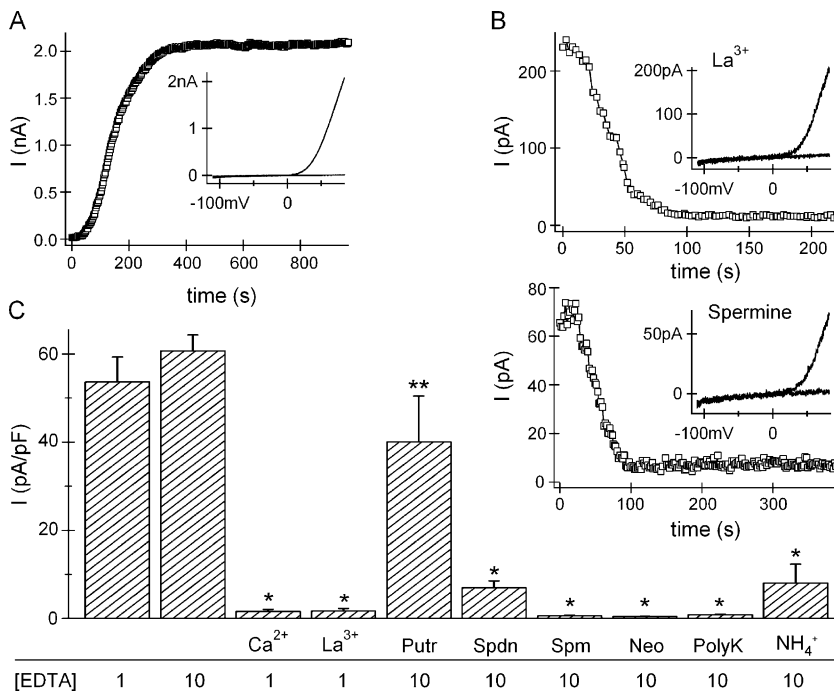
Figure 1. Inhibition of MIC current by internal polyvalent cations and NH_4^+. RBL cells with standard internal solution and 2 Ca^{2+} external solution. All current amplitudes were measured at +85 mV during voltage ramp stimuli. (A) Time course of I_{MIC} development during whole-cell recording and dialysis with 10 mM EDTA. Outward MIC current amplitude is plotted against time after break-in. The inset shows I-V relations obtained at break-in and after 10 min of recording. (B) The time course of inhibition of preactivated MIC current by La^{3+} (top). The pipette solution contained 1 mM EDTA + 3 mM La^{3+}. The inset shows the I-V relation at break-in and after complete inhibition. The bottom panel shows the time course of inhibition of preactivated MIC current by spermine. The pipette solution contained 10 mM EDTA + 5 mM spermine. The inset shows I-V relations obtained at break-in and after complete inhibition. (C) Maximal current densities with control (1 mM, $n = 5$ cells) or 10 mM EDTA ($n = 3$) solutions and with solutions containing inhibitory cations. The cation concentrations in mM were: 5 Ca^{2+} ($n = 5$); 3 La^{3+} ($n = 8$); 8 putrescine ($n = 4$); 5 spermidine ($n = 5$); 4 spermine ($n = 5$); 6 neomycin ($n = 5$); 4 polylysine ($n = 6$); 112 NH_4^+ ($n = 5$). *, P < 0.005 compared with controls in 1 or 10 mM EDTA. **, P = 0.16.

Distinguishing Inhibition from Block of MIC Current

Internal metal cations and polyamines at partial blocking concentrations did not affect the MIC I-V shape in either Ca^{2+}-containing or divalent-free external solution (unpublished data), consistent with previous observations with 300 μM internal spermine (Kerschbaum et al., 2003). In contrast, strongly voltage-dependent pore block was observed with external Mg^{2+} and polyamines in the micromolar range (Kozak et al., 2002; Kerschbaum et al., 2003). Fig. 2 compares monovalent I-V relations obtained in a T cell at break-in (red traces) and after full current development in the absence of external divalents when the internal solution contained NH_4^+, tetraethylammonium, or tetramethylammonium (20 mM each). Internal NH_4^+ did not alter the I-V shape (compare Fig. 2, A and B), although it inhibited I_{MIC} (Fig. 1 C). In contrast, TEA and TMA (Fig. 2, C and D) preferentially blocked the outward current, consistent with a previous report (Gwanyanya et al., 2004), but did not inhibit inward currents. To examine the steepness of voltage-dependent block, Boltzmann fits of blocked to unblocked current ratios gave electrical distance values (δ, from the inside) that averaged 0.23 for TMA ($n = 3$) and 0.3 for TEA ($n = 3$). However, pore block and channel inhibition appear to be unrelated. For example, TMA at concentrations of up to 112 mM, a concentration sufficient to block most of the outward current, had no effect on current

amplitude assessed at negative potentials ($n = 5$, unpublished data). Thus, NH_4^+ is an inhibitor but not a pore blocker, whereas TMA or TEA are pore blockers that do not inhibit MIC channels.

As a further test of the requirements for charge screening to produce inhibition (not block) of I_{MIC}, we tested the effect of hexamethonium, a divalent ion whose charges are separated by ∼10 Å (Alvarez et al., 1983). Unlike divalent cations with higher charge density, hexamethonium (16 mM, $n = 4$) produced only voltage-dependent block of outward currents (Fig. 2 E), and did not inhibit inward current development (Fig. 2 F). To date, we have found no cation that can both block and inhibit I_{MIC}.

Comparison with Inward Rectifier K⁺ Channel

$PI(4,5)P_2$, an anionic phospholipid (−3 residual charges) residing primarily in the inner leaflet of the plasma membrane, is known to interact electrostatically with various membrane proteins, including ion channels (Hilgemann and Ball, 1996; Langner and Kubica, 1999; McLaughlin et al., 2002). We next compared regulation of MIC with the endogenous inwardly rectifying K⁺ channel (IRK1) in RBL cells, the activity of IRK1 being used essentially as a "bioassay" of membrane-associated PIP_2 (see Huang et al., 1998; Kozak et al., 2002). Fig. 3 A illustrates the time courses of MIC and IRK1 current development recorded simultaneously in an
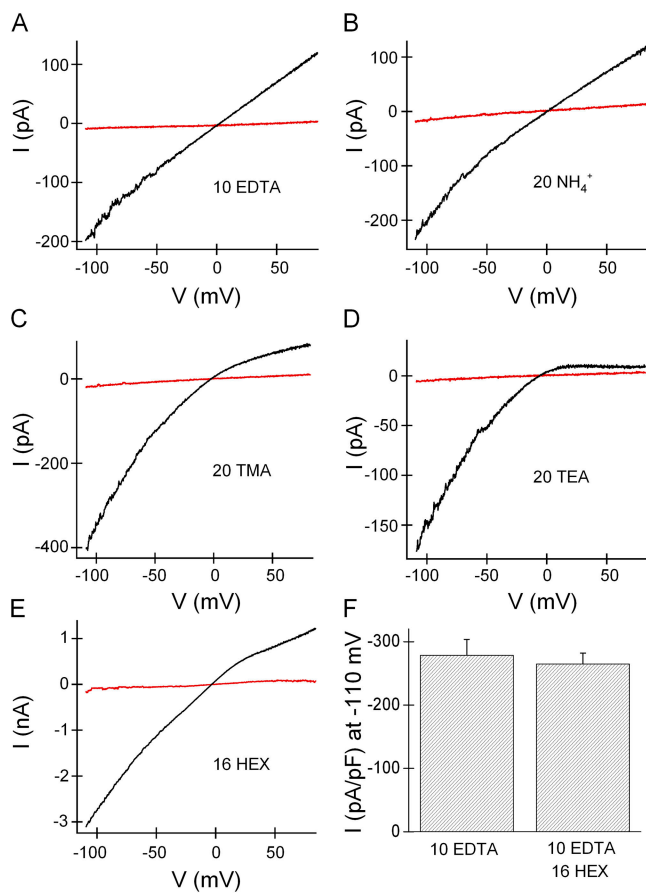
Figure 2. Block of outward MIC current by internal quaternary ammonium derivatives and hexamethonium. Human resting T cells (A–D) and RBL cells (E and F) with 130 mM Cs^+ glutamate, 8 mM NaCl, 10 mM EDTA, 0.9 mM $CaCl_2$, 10 mM HEPES, pH 7.3; and 10 HEDTA-Cs^+ (A–D) and 1 HEDTA-Cs^+ (E and F) external solution. Divalent-free external solution permits inward monovalent current recording. I-V relations were obtained at break-in (red traces) and after full development of the current with internal solutions containing no blocker (A) or 20 mM NH_4^+ (B), TMA (C), TEA (D), and hexamethonium (E). TMA, TEA, and hexamethonium, but not NH_4^+, produced voltage-dependent block of the outward MIC current. (E) Inward MIC current in the presence and absence of 16 mM hexamethonium. The values are not statistically different (P > 0.05).

RBL cell using K^+ as the main internal cation. Neomycin (3 mM) inhibited both MIC and IRK1 currents from the inside, as seen in Fig. 3 B. It is apparent that IRK1 current is inhibited more slowly than the MIC current. Fig. 3 C shows the I-V relations obtained at the time points indicated in Fig. 3 B. The outward K^+ current through IRK1 channels is blocked to a greater degree than the inward K^+ current (compare color traces 1 and 2). In this case, voltage-dependent block by neomycin from the inside can be detected because the current has not yet been fully inhibited. IRK1 channel block by neomycin is qualitatively reminiscent of internal polyamine block underlying the inward rectifica-

tion of IRK family channels (Lopatin et al., 1994; Fakler et al., 1995; Guo and Lu, 2000). Thus, the inhibition by neomycin proceeds with a very slow time course after its arrival near the channel protein. Similar results were seen with poly-L-lysine (unpublished data). In conclusion, the cationic compounds that are expected to screen PIP_2 negatively charged head groups inhibit both MIC and IRK1 currents, although MIC current inhibition has a more rapid time course.

### Effects of Altered Internal pH on MIC Current Activation and Inhibition

Activation by External NH_4^+. NH_4^+ ions are permeant and carry significant inward current through the MIC channel in the absence of divalent cations (Kozak et al., 2002). While recording from RBL cells with millimolar internal Mg^{2+} to inhibit I_{MIC}, we found that a current with identical I-V characteristics was activated by external NH_4^+. Fig. 4 A shows a recording from an RBL cell with 5 mM internal Mg^{2+}. As expected, I_{MIC} failed to develop. However, when external Na^+ was exchanged for NH_4^+, I_{MIC} developed gradually, relieving inhibition by internal Mg^{2+}. The effect of NH_4^+ was reversible; upon removal of external NH_4^+ the current was again inhibited. When internal Mg^{2+} was higher (8–10 mM), NH_4^+ had a greatly reduced effect (unpublished data). In RBL cells that displayed preactivated MIC current, external NH_4^+ also abolished the inhibition by internal Mg^{2+} (Fig. 4 B). Upon removal of NH_4^+, current decreased as inhibition by Mg^{2+} returned. Activation by external NH_4^+ was repeated for several cycles. We conclude that external NH_4^+ permits I_{MIC} development in the presence of inhibitory $[Mg^{2+}]_i$ and reversibly prevents inhibition of the preactivated current.

We sought to explain the activation of I_{MIC} by external NH_4^+ by its expected ability to elevate internal pH (Boron et al., 1978; Roos and Boron, 1981; Boron, 1983). NH_4^+ is in equilibrium with its freely membrane-permeant neutral form NH_3 (Antonenko et al., 1997). From the Henderson-Hasselbalch equation, 81 mM NH_4^+ at pH 7.4 includes ~0.8 mM NH_3. NH_3 would enter the cell, capture a proton, and thus make the internal pH more alkaline. To understand the effect of external ammonium to antagonize or reverse the inhibition of MIC current by Mg^{2+} we asked several additional questions.

Is the NH_4^+ effect concentration dependent, can it proceed in the absence of internal Mg^{2+}, and are the kinetics consistent with an internal or external site of action? Fig. 5 A shows that application of external NH_4^+ at increasing concentrations (20, 81, and 162 mM) resulted in increased MIC current amplitude following full development in the absence of internal Mg^{2+}. Although dose dependent, the increase in current was not rate limited by the speed of NH_4^+ application; as shown in
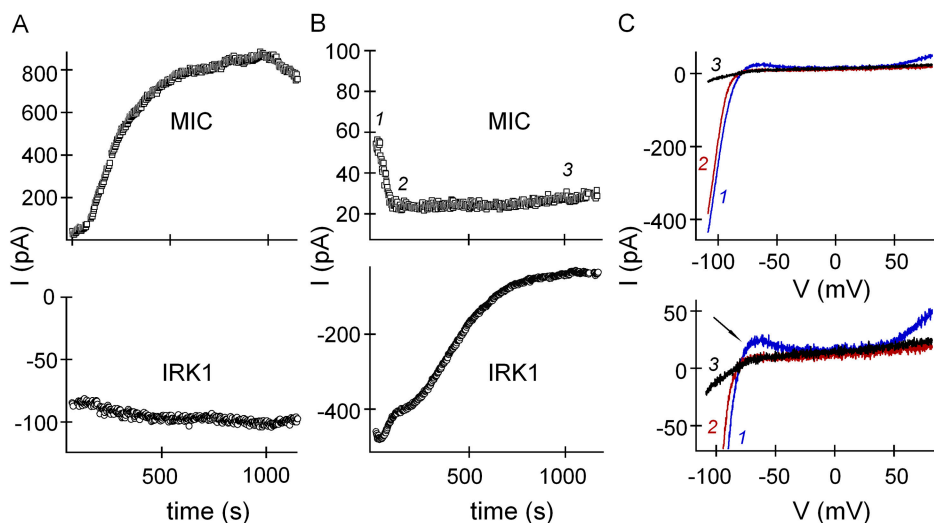
Figure 3. Neomycin inhibition of MIC and IRK1 currents. RBL cells with 10 mM EDTA-containing internal solution and 4.5 K^{+}, 2 Ca^{2+} external solution. (A) Time course of development of MIC (measured at +85 mV) and IRK1 (measured at −110 mV) currents. (B) Neomycin (3 mM) inhibits preactivated MIC and IRK1 currents from inside. (C) I-V relations obtained from B at times 1–3. The plot on top is enlarged below to show that neomycin block precedes its inhibition of IRK1 current. The red trace shows blocked (but not inhibited) IRK1 current. The arrow indicates outward IRK1 current that is rapidly blocked by neomycin diffusing into the cell.
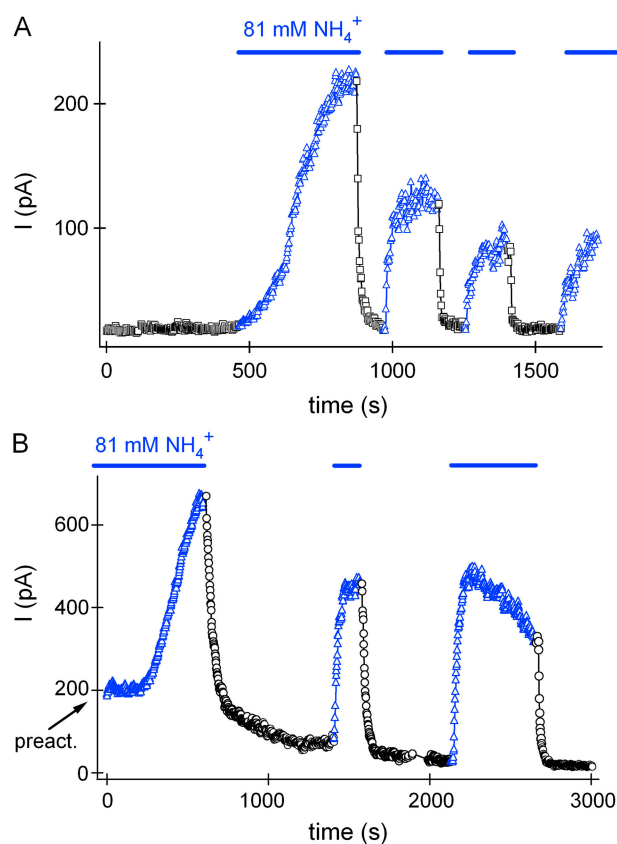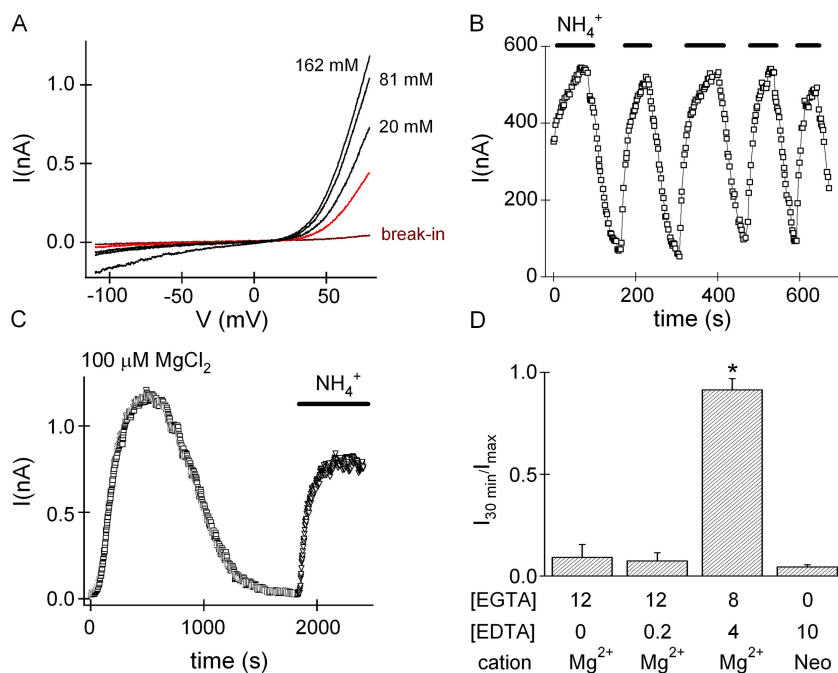

Figure 4. External NH_4^+ effect on MIC current in the presence of internal Mg^{2+}. RBL cells in 2 Ca^{2+} external solution. (A) The internal solution contained 12 mM EGTA and 5 mM $MgCl_2$ ($[Mg^{2+}]_{free}$ = 3 mM). Application of external 81 mM NH_4^+ reversed inhibition by internal Mg^{2+} in several successive trials; Mg^{2+} inhibition was reestablished upon washout of NH_4^+. (B) NH_4^+ prevents inhibition of preactivated MIC current by 2.3 mM free Mg^{2+} (12 mM EGTA + 4 mM $MgCl_2$).

Fig. 5 B, the increases in current upon exposure to external NH_4^+ were rather slow and reversible. These results are consistent with NH_4^+ acting by increasing cytosolic pH, a process expected to be slower than direct binding of NH_4^+ to a low-affinity external site on the channel.

We also tested if external NH_4^+ promotes recovery of I_{MIC} after rundown. Fig. 5 C shows I_{MIC} development and subsequent complete rundown with 54 μM free internal Mg^{2+}. Subsequent application of external NH_4^+ resulted in recovery from current rundown. The recovery of current by NH_4^+ demonstrates that rundown does not reflect the disappearance or degradation of channels from the plasma membrane. Since NH_4 efficiently reversed inhibition in the presence of millimolar internal Mg^{2+} (Fig. 4), we sought to determine if rundown is also Mg^{2+} dependent and if it can be prevented by reducing internal Mg^{2+}. Fig. 5 D shows that this is the case; 54 μM internal Mg^{2+} (with an EGTA-containing solution) caused nearly complete rundown. Addition of 200 μM EDTA, a chelator with a higher Mg^{2+} affinity to reduce free Mg^{2+} to 2 μM, did not significantly alter the extent of rundown. However, the current was completely rescued from rundown by the addition of 4 mM EDTA that reduces the internal free Mg^{2+} to ~52 nM. Thus, we demonstrate that rundown is produced by low micromolar levels of internal Mg^{2+} and can be reversed by NH_4^+ application, which elevates internal pH. However, cytoplasmic alkalinization did not completely abolish rundown; at longer times, I_{MIC} ran down even in the presence of external NH_4^+ (81 mM, unpublished data). Mg^{2+} was not unique in its ability to promote current rundown. Inclusion of 500 μM neomycin in the pipette solution containing 10 mM EDTA and no Mg^{2+} also caused rundown (Fig. 5 D).

In addition to its effects on MIC channels, external NH_4^+ reversibly activated a small, linear conductance in RBL cells. This conductance, unlike I_{MIC}, was not
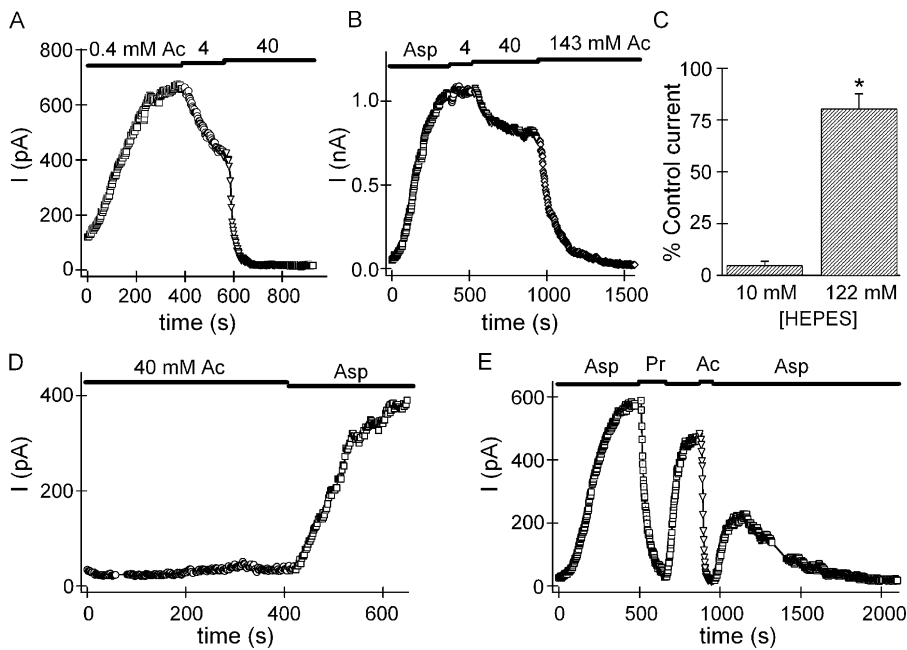
Figure 5. Effect of external NH_4^+ on MIC current in the absence of internal Mg^{2+}: recovery from rundown. RBL cells in 2 Ca^{2+} external solution with 12 mM EGTA internal solution. (A) MIC current was allowed to develop, and I-V plots obtained at break-in and after the current was fully developed (shown in red color). NH_4^+ at varying concentrations (20 mM, 81 mM, and 162 mM) was applied subsequently and I-V plots are shown. Note the inward current activated in external NH_4^+-containing solution. (B) Rapid application of 81 mM NH_4^+ causes reversible slow potentiation of the MIC current. (C) MIC current development and rundown. 12 mM EGTA, 100 μM $MgCl_2$ internal solution, $[Mg^{2+}]_{free}$ = 54 μM. 81 mM NH_4^+ applied after rundown resulted in recovery of I_{MIC}. (D) Dependence of MIC current rundown on Mg^{2+} and neomycin. Current amplitude (+85 mV) was obtained 30 min ($I_{30 min}$) after break-in, divided by maximal amplitude (I_{max}) in the same cell, and the ratio plotted for 12 mM EGTA (free Mg^{2+} = 54 μM; n = 10 cells), 12 mM EGTA + 0.2 mM EDTA (free Mg^{2+} = 2 μM, n = 5), 8 mM EGTA + 4 mM EDTA (free Mg^{2+} = 52 nM, n = 7) and 10 mM EDTA+ 500 μM neomycin (n = 3) internal solutions. *, P < 0.005 compared with the value for 2 μM free Mg^{2+}.

sensitive to cytosolic Mg^{2+} or external divalent cations. It reversed above +40 mV and can be seen in Fig. 5 A as an inward current at negative membrane potentials. The current amplitude increased with increasing NH_4^+ concentrations above 20 mM; at NH_4^+ concentrations of ∼80 mM, the current did not contaminate the outward MIC current significantly. The nature of this conductance was not investigated further, but it may represent an NH_4^+-activated current previously described in *Xenopus* oocytes (e.g., Boldt et al., 2003).

Does Internal Acidification by a Weak Acid Inhibit MIC Current? Effects of Altered Internal pH Buffering. The experiments described above employed aspartate as the main external anion. Weak acids, such as acetate and propionate, applied externally are known to reduce the intracellular pH by diffusing through the membrane in the neutral form and then dissociating to release protons (Boron, 1986). We therefore tested if these weak acids influenced MIC channels by increasing proton concentrations at the cytosolic side of the membrane. Using a Mg^{2+}-free pipette solution, MIC current was first allowed to develop for 6–10 min in external aspartate supplemented with 0.4 mM acetate (Fig. 6 A). Upon maximal activation of the current, the external acetate concentration was increased to 4 and then 40 mM, resulting in a dramatic reduction of I_{MIC}. In most RBL cells, 40 mM external acetate was sufficient to inhibit I_{MIC} completely despite the complete absence of internal divalents.

We next tested if the inhibitory action of external acetate is mediated through a reduction in internal pH. If this were true, then increasing the pH-buffering capacity of the pipette solution would be expected to counteract the effects of acetate. Fig. 6 (A and B) directly compare I_{MIC} inhibition induced by acetate when the pipette contained 10 mM or 122 mM HEPES. Even though the acetate effect was not abolished by increased buffering, a higher concentration (143 mM) was necessary for complete inhibition of the current. Fig. 6 C summarizes the data for 40 mM acetate; increasing the internal HEPES concentration 10-fold nearly abolished the inhibitory effect of external acetate, strongly supporting the conclusion that cytosolic acidification inhibits MIC current. In another set of experiments, we showed that MIC current did not develop in RBL cells bathed in acetate (40 mM) before the start of recording; I_{MIC} failed to develop even though cell dialysis with a Mg^{2+}-free solution continued for minutes (Fig. 6 D). After 6 min, a time of dialysis normally sufficient for full I_{MIC} activation in nonacetate solutions, the external anion was switched to aspartate and a robust MIC current was activated. The time course of development was not instantaneous, however. According to our interpretation, cell dialysis with a Mg^{2+}-free solution renders MIC channels available for opening, but acetate prevents their opening by acidifying the internal pH. We also tested if external acetate is unique in its inhibitory action. Propionate (40 mM) in

Figure 6. Effects of external acetate ion on MIC current in RBL cells. (A) MIC current inhibition by application of external acetate when internal solution contained 10 mM HEPES. (B) Increasing internal pH buffering with 122 mM HEPES shifts the acetate effect to higher concentrations. (C) Summary of 40 mM acetate inhibition of MIC current with 10 mM ($n = 5$) or 122 mM ($n = 3$) HEPES in the pipette (*, P < 0.005 compared with the value obtained with 10 mM HEPES). The current amplitude was measured at 360 s after the start of acetate application, divided by the amplitude immediately before acetate addition, and plotted as percent of control current. (D) MIC current fails to develop with 0 Mg^{2+} inside in the presence of external 40 mM acetate. Upon washout of acetate, the current developed normally. (E) Reversible MIC current inhibition by propionate (40 mM) and acetate (40 mM) in the same cell. After prolonged dialysis, the current ran down completely in the absence of external acetate. MIC current amplitudes were measured at + 85 mV.

the external solution was also effective in completely inhibiting the current (Fig. 6 E). The speed or extent of current rundown was not affected noticeably by propionate or acetate treatment. Acetate and propionate were also effective in Jurkat T cells and human T cells. Formate, methanesulfonate, citrate, and glutamate solutions exhibited no inhibitory effect (unpublished data). The inhibitory effect is thus confined to weak acids that are known to produce cytosolic acidification when applied externally (Stewart et al., 2002).

### Activation of MIC Channels during Perforated-patch Recording

The activation of MIC current in native cells is normally observed only during prolonged whole-cell recording.

Preactivated I_{MIC} at break-in is small or absent, and I_{MIC} does not develop during perforated-patch recording (Jiang et al., 2003). Fig. 7 shows a perforated-patch recording of I_{MIC} in an RBL cell. No current was present for ~6 min in normal external (Na^+) solution. However, following application of NH_4^+ (81 mM), I_{MIC} began to develop (Fig. 7 A). The I-V relation in NH_4^+ (Fig. 7 B) is indistinguishable from I-Vs obtained in whole-cell recording. The current started to decline upon NH_4^+ washout, and declined more rapidly when external 40 mM propionate was applied (Fig. 7 A). The effect of NH_4^+ was reversible and could be repeated in the same experiment. This demonstrates that MIC current can be activated by cytosolic alkalinization without whole-cell dialysis.
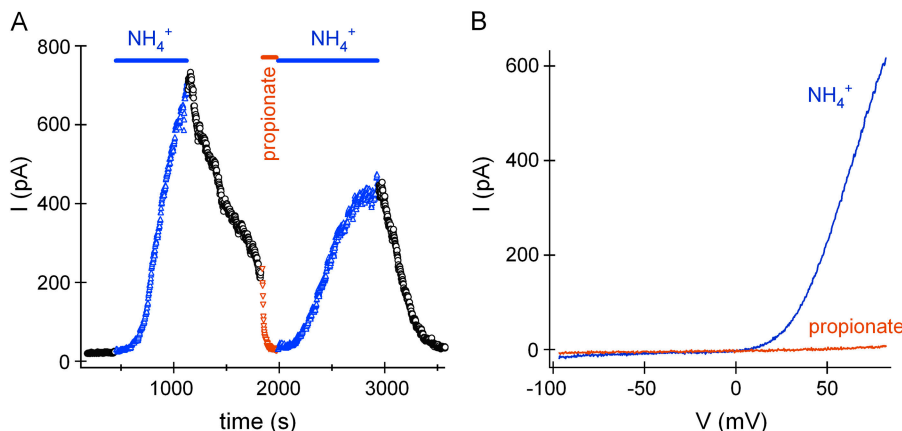
Figure 7. Activation of MIC current by NH_4^+ in perforated-patch recording. RBL cell in 2 Ca^{2+} external solution; amphotericin B–containing pipette solution. (A) MIC current failed to develop during recording before application of external 162 NH_4^+ which resulted in the development of a robust current. I_{MIC} declined slowly upon removal of NH_4^+ and rapidly upon addition of 40 mM propionate-containing solution. Both propionate and NH_4^+ effects were reversible. (B) I-V relations obtained from the experiment shown in A in the presence of external NH_4^+ and propionate.
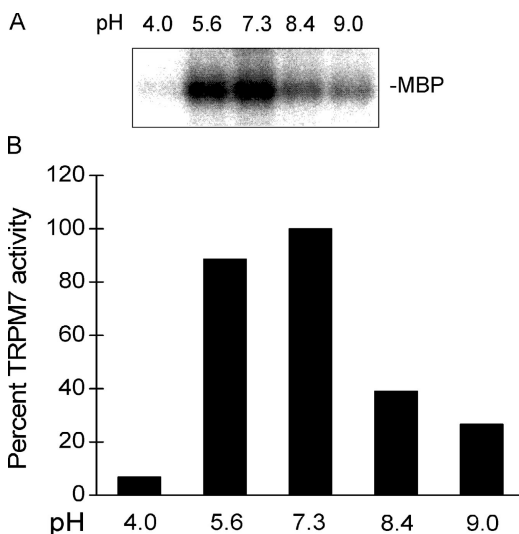
Figure 8. pH dependence of TRPM7 kinase domain phospho-transferase activity. (A) TRPM7 kinase domain phosphorylation of MBP (myelin basic protein) was assessed in vitro at various pH values. The panel shows an autoradiogram of radioactive ATP-labeled MBP after phosphorylation in buffer at various pH values. (B) The kinase activity of TRPM7 was quantified by comparing the intensity of the P^{32} signal shown in A. Band intensity at 7.3 was set as 100%. The activity was substantially reduced at pH 4.0 and 9. The figure is representative of three separate experiments.

pH Dependence of Recombinant TRPM7 Kinase and Channel Activities

We further investigated effects of pH on the channel activity of expressed TRPM7 and also on the intrinsic kinase activity of TRPM7. We began by characterizing the pH sensitivity of murine TRPM7 kinase domain purified from *E. coli* (Fig. 8). As shown previously, the kinase domain has phosphotransferase activity in vitro and phosphorylates MBP and autophosphorylates on two identified serine residues (Ser1511 and Ser1567; Matsushita et al., 2005). Fig. 8 A shows that kinase activity is optimal near the physiological pH of 7.3, with MBP as a substrate. The band intensity is maximal at normal pH (7.3) and is reduced at alkaline (pH 8.4, 9.0) and very acidic (pH 4.0) pH values (Fig. 8 B).

Like native MIC channels, heterologously expressed TRPM7 is inhibited by internal Mg^{2+} (Nadler et al., 2001). To examine whether the recombinant channel is also sensitive to pH_i, we used whole-cell and inside-out patch recording and compared the pH dependence of channel activity with that of its kinase activity. Whole-cell dialysis using a Mg^{2+}-free solution at pH 7.3 would normally greatly enhance the TRPM7 current. However, the current was completely inhibited by dialysis with acidic pH (Fig. 9, A and B). In control or transfected CHO cells, dialysis with acidic solutions (pH below 6) activated a small (~150 pA at +85 mV) outward current that peaks at ~100 s in Fig. 9 A. This
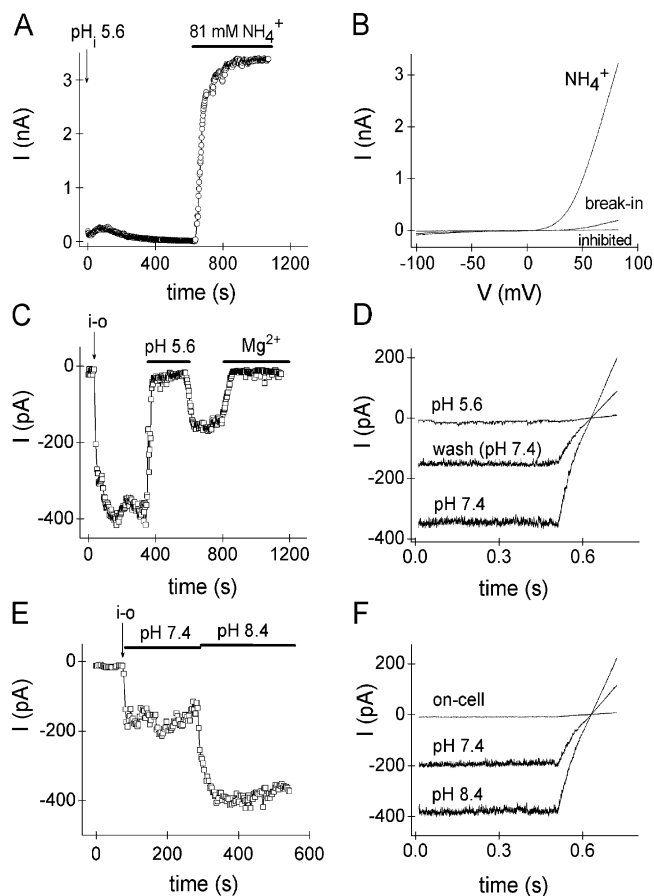
Figure 9. The pH_i dependence of recombinant TRPM7 in whole-cell and inside-out patch recordings. (A) Time course of internal pH inhibition and recovery by external NH_4^+ during whole-cell recording of overexpressed mTRPM7 in a CHO cell. pH 5.6 internal solution; 2 Ca^{2+} external solution. Whole-cell recording was initiated at arrow. TRPM7 current amplitude was measured at +85 mV. (B) Individual I-V traces obtained from A. (C) Inside-out patch recording; time or patch excision indicated by arrow. Pipette and bath solutions were 1 mM HEDTA, 154 mM Cs^+ aspartate to minimize rundown. Divalent-free external solution permits inward monovalent current recording. pH 5.6 at cytoplasmic surface inhibited TRPM7 fully and reversibly. In the same patch, 2 mM $MgCl_2$ also inhibited the current. (D) Currents at −100 mV and during voltage ramps to +85 mV. (E and F) Increasing the pH from 7.4 to 8.4 increased TRPM7 current amplitude in inside-out patches.

current ran down 3–4 min after break-in and most probably represents a voltage-activated proton conductance present in the CHO cell line (Cherny et al., 1997). The inhibition of TRPM7 channel activity by acidic internal pH was overcome by external NH_4^+. External NH_4^+ did not alter the TRPM7 I-V shape in the presence of external divalent cations. The effects of pH_i and $NH_4^+{}_o$ on the expressed TRPM7 current are therefore similar to effects on the endogenous MIC current.

To compare pH and Mg^{2+} effects on recombinant TRPM7 channels more directly, we recorded from in-
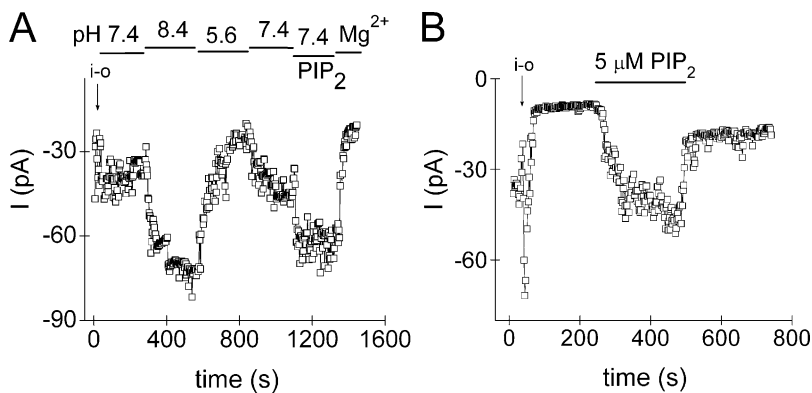
Figure 10. PI(4,5)P$_2$ and pH effects on TRPM7 current in inside-out patch. CHO cell overexpressing mTRPM7. Divalent-free external solution permits inward monovalent current recording. (A) Pipette and bath contained 1 mM HEDTA, 154 mM Cs$^+$ aspartate. pH 8.4 increased current whereas pH 5.6 completely inhibited it. 5 μM PIP$_2$-diC8 application in pH 7.3 mimicked the effect of increased pH. 2 mM MgCl$_2$ was applied. (B) Bath solution contained Cs$^+$ glutamate, 10 EGTA. Establishment of inside-out configuration (i-o) resulted in increased current due to Mg^{2+} washout followed by rapid rundown. Application of 5 μM PIP$_2$-diC8 to the cytosolic side of the membrane resulted in TRPM7 current recovery.

side-out patches (Fig. 9, C and D). At the arrow, the patch was excised into a divalent-free solution at pH 7.3 and monovalent TRPM7 current recorded. Direct exposure to pH 5.6 inhibited the current completely and reversibly. In the same patch, millimolar Mg^{2+} also abolished TRPM7 current. Fig. 9 (E and F) shows that increasing cytosolic pH from 7.4 to 8.4 enhanced TRPM7 current substantially, in qualitative agreement with our findings on native MIC current (Fig. 5) and TRPM7 whole-cell recordings (Fig. 9, A and B).

In summary, overexpressed TRPM7 channels are inhibited by acidic pH and potentiated by basic pH. The pH dependence of the channel activity is distinguishable from effects on the intrinsic kinase activity; pH 8.4 increases channel activity but decreases kinase activity, whereas pH 5.6 reduces current activity yet has almost no effect on kinase activity.

Comparison of diC8-PIP$_2$ and Altered pH in Inside-out Patches

Runnels et al. (2002) demonstrated that heterologously expressed TRPM7 channels are targets of PI(4,5)P$_2$ activation. Recently, Takezawa et al. (2004) questioned the role of PIP$_2$ on TRPM7 and showed that overexpression of TRPM7 disrupts PIP$_2$ signaling. We explored the effects of pH, PIP$_2$, and Mg^{2+} on the same population of channels in inside-out patch recordings from cells expressing TRPM7. Fig. 10 A first shows TRPM7 current at normal pH (7.4). Increasing pH to 8.4 increased the current substantially (see also Fig. 9 E), whereas acidic pH (5.6) completely inhibited the current (see also Fig. 9 C). Inhibition was readily reversed by returning to normal pH. Addition of diC8-PIP$_2$ to the bath increased channel activity close to that observed at pH 8.4, whereas subsequent addition of Mg^{2+} completely inhibited the current. Therefore, PIP$_2$ was effective in recombinant TRPM7-overexpressing cells and mimicked the effect of cytosolic alkalinization in the same membrane patch. In Fig. 10 B, the patch was excised into a solu-

tion promoting rundown (10 EGTA). After disappearance of channel activity, 5 μM diC8-PIP$_2$ applied to the cytoplasmic side of the membrane caused recovery from rundown. The PIP$_2$ effect was partially reversible upon washout. Application of phosphatidyl serine (200 μM) was not effective (unpublished data). Together, these experiments demonstrate that increased pH and exogenously added PIP$_2$ have similar effects on current amplitude and recovery from rundown.

If, as suggested by Fig. 10, increasing TRPM7 current in pH 8.4 is similar in nature to increasing PIP$_2$ concentration, we would also expect increased pH by itself (with no added PIP$_2$) to promote recovery from rundown. Fig. 11 A shows that this is the case. TRPM7 monovalent current first activated upon patch excision into EGTA-containing solution at pH 7.3 and then ran down completely. Exposure to pH 8.4 produced robust current activation (see Fig. 11 B for corresponding I-V curves). The current was then completely inhibited upon returning to pH 7.3.

We next tested if cytosolic acidification affects basal channel activity present in cells expressing recombinant TRPM7. Fig. 11 (C and D) shows a cell-attached recording with constitutively active channels. Upon addition of acetate to the bath, the ~40 pS channels are inhibited reversibly, demonstrating that the cytosolic pH dependence of TRPM7 channel activity is present in an intact cell. We also tested if TRPM7 phosphotransferase activity is necessary for the pH effects on the current. Fig. 11 (E and F) shows channel activity of a "kinase-dead" (TAP, D1775A) point mutant during cell-attached recording from a transfected CHO cell. Application of external acetate completely and reversibly inhibited the current (Fig. 11 F). The pH dependence of the TRPM7-TAP mutant and the double autophosphorylation mutant was also similar to WT TRPM7 (whole-cell recording; unpublished data). We conclude that phosphorylation by TRPM7 or a functioning kinase domain are not likely to influence the pH dependence of TRPM7 current.
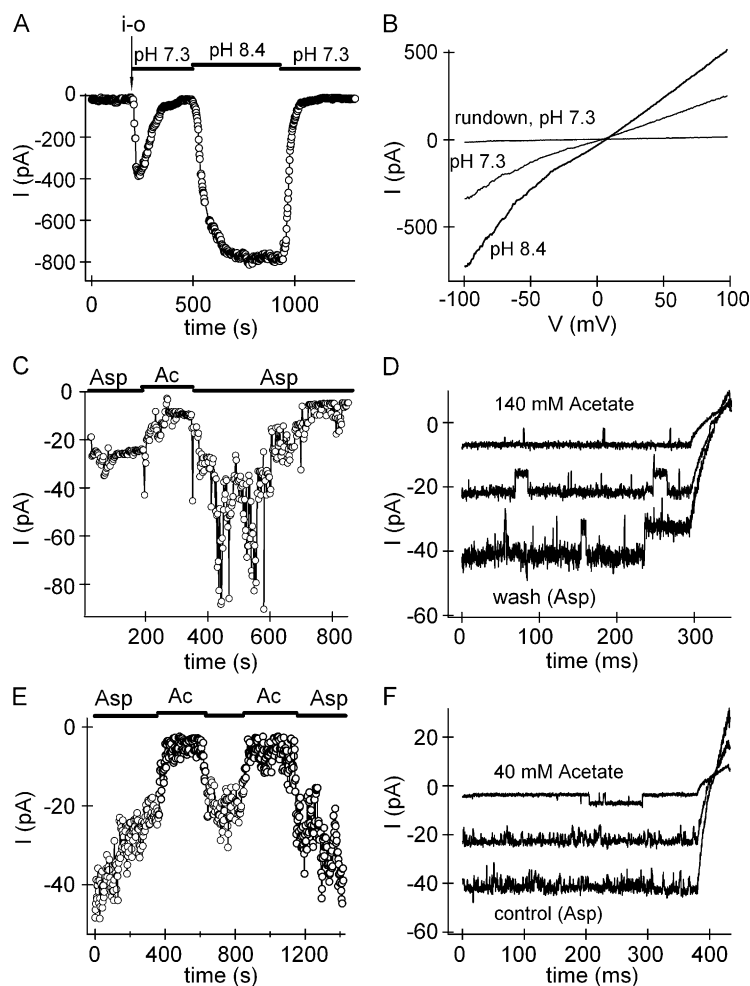
Figure 11. TRPM7 current recovery from rundown; inhibition in cell-attached mode. CHO cells overexpressing mTRPM7 WT and TAP mutant. (A and B) Inside-out patch. Monovalent TRPM7 current was allowed to run down fully in 1 mM EGTA, pH 7.3 bath solution. Current recovered and was potentiated by applying pH 8.4 solution to the cytosolic side. Upon return to pH 7.3, the current was inhibited again (compare with Fig. 5 C). (C and D) Cell-attached patch. Sensitivity of I_{TRPM7} to internal pH changes. The basal $\sim$40 pS channel activity was inhibited when bath solution was switched from aspartate to acetate in order to acidify the cytosol of the intact cell. The acetate effect was reversible. (E) Sensitivity of $I_{TRPM7\text{-}TAP}$ (kinase-dead mutant) to internal pH changes in the cell-attached mode. Constitutive activity of TRPM7-TAP channels was monitored in cell-attached patch in 2 Ca^{2+} bath solution. Repeated addition of 40 mM acetate to the bath inhibited channel activity. (F) Traces from experiment shown in E. The current trace in the middle represents current before acetate application.

DISCUSSION

The aim of this study was to investigate the nature of internal Mg^{2+} inhibition of MIC and TRPM7 channels. Our results can be summarized by three main points. (1) We demonstrate that a wide variety of internal cations, metal and organic (even ammonium), can inhibit MIC current by a mechanism that has slow kinetics, does not involve direct pore block, and is independent of kinase activity. (2) We show that MIC current can be activated by elevated internal pH, despite the presence of internal Mg^{2+} (or other endogenous cations). (3) Using heterologously expressed TRPM7, we show that inhibition of the current at low cytoplasmic pH occurs by screening the negatively charged head groups on $PI(4,5)P_2$ or another acidic lipid. Conversely, alkaline pH is able to potentiate TRPM7 current and bring about recovery from rundown, similar to PIP_2 effects on the same channels. These results are consistent with a charge-screening mechanism in which any of several cations can inhibit channel activity by binding to PIP_2. Lowering internal Mg^{2+} is neither necessary nor sufficient to activate MIC/TRPM7 current, since alkaline pH can activate the current without changing Mg^{2+},

and acidic pH or polyamines can inhibit when Mg^{2+} is chelated.

The Nature of Mg^{2+} Inhibition: Kinase-mediated or Charge Screening?

Previous reports have shown that Mg^{2+} and Mg^{2+}-ATP inhibit the TRPM7 current and suggested that channel activity is regulated by a site within the kinase domain (Nadler et al., 2001; Schmitz et al., 2003). Mg^{2+} in the millimolar range inhibits channel activity but also enhances the kinase activity of TRPM7. Based on this Mg^{2+} dependence and studies of kinase-domain mutants, Schmitz et al. suggested that the two Mg^{2+} effects are connected; according to this view, increased kinase activity would inhibit channel activity (Schmitz et al., 2003). However, we have shown that Mg^{2+} is not unique in inhibiting the MIC channel; other divalent metal cations such as Zn^{2+}, Mn^{2+}, Sr^{2+}, and Ba^{2+} also inhibit at millimolar concentrations (Kozak and Cahalan, 2003). In contrast, block is rapid and voltage dependent. Moreover, the cations that are channel pore blockers failed to inhibit the MIC current (see Fig. 2, E and F). The mechanism of inhibition has remained controversial until now.

The kinase domain of TRPM7 has Mg^{2+}- and nucleotide-binding domains as do other eukaryotic protein kinases (Yamaguchi et al., 2001; Manning et al., 2002b). Nadler et al. (2001) found that other nucleotides such as MgGTP or MgCTP also inhibited TRPM7 current at millimolar concentrations. MgGTP can substitute in many cases for MgATP as the donor of the γ-phosphate for the phosphotransferase activity (Hanks and Hunter, 1995). But TRPM7 (kinase) can only utilize MgATP (Ryazanova et al., 2004). Pyrimidines, such as MgCTP, cannot be used by eukaryotic protein kinases in the place of MgATP (Hanks and Hunter, 1995; Gomperts et al., 2003). Therefore the findings of Nadler et al. contradict the idea that the Mg^{2+}-nucleotide binding region within the kinase domain is a site of channel inhibition. Furthermore, using chelators to maintain constant free Mg^{2+} levels while varying Mg^{2+}-ATP, we were able to show that Mg^{2+} ion alone, but not MgATP, is the species that inhibits the MIC channel (Kozak and Cahalan, 2003).

In a recent study, we approached the question of Mg^{2+} inhibition by using site-specific mutations of the TRPM7 kinase domain, as Schmitz and colleagues had done. "Kinase-dead" and autophosphorylation-resistant mutations in the TRPM7 protein did not alter Mg^{2+} sensitivity of channel activity (Matsushita et al., 2005). Additionally, the kinase-dead mutation (Fig. 11, E and F) and the double autophosphorylation mutations (unpublished data) did not alter the pH dependence of the current, and the kinase-deletion mutant did not exhibit increased channel activity above background upon NH_4^+ application (unpublished data). These results suggest that even though the kinase activity of TRPM7 is divalent metal cation sensitive (like many other eukaryotic kinases; Ryazanova et al., 2004), the inhibitory effect of Mg^{2+} on channel current represents a completely different site of action. Thus, we showed that kinase and channel activities could be dissociated by using differences in metal cation sensitivity of the kinase and the channel activities. Furthermore, TRPM7 current is inhibited equally well by Zn^{2+} and Ca^{2+}, yet they either inhibit or have no effect on the kinase activity, respectively (Matsushita et al., 2005). In experiments presented here, we demonstrate that pH also differentially affects channel and kinase activities; alkaline pH (8.4) inhibits TRPM7 kinase activity by >60% but increases channel current (Figs. 8 and 9). Thus, in our hands, kinase activity and channel activity are separable by differential effects of mutations, divalent cations, and pH. The possible function of the TRPM7 kinase remains unknown.

Several cation channels have been shown to exhibit internal Mg^{2+} inhibition similar to that described in this study. Yazejian and Byerly (1989) and Strong and Scott (1992) showed that a nonselective cation channel found in *Lymnaea* neurons can be activated upon patch excision. This "HP channel" conducts Ca^{2+}, Mg^{2+}, and Ba^{2+}, shows steep outward rectification, and is inhibited by millimolar concentrations of internal Mg^{2+}, Ba^{2+}, and Sr^{2+} (Yazejian and Byerly, 1989). The Mg^{2+} inhibition was reversible in inside-out patch recording and distinct from an open channel Mg^{2+} block. The primary effect of internal Mg^{2+} was a marked reduction of opening probability (Strong and Scott, 1992). The molecular identity of the HP channel is still unknown. In *C. elegans*, a current resembling MIC has been characterized recently and named I_{ORCa} (Estevez et al., 2003). Its main biophysical characteristics are similar to MIC/TRPM7; importantly, internal Mg^{2+} inhibits the channels in a voltage-independent manner, yet MgATP has no additional effect. Interestingly the *C. elegans* genome has only one eEF2 kinase family member and it is not fused to an ion channel domain (Manning et al., 2002a). This implies that the Mg^{2+} inhibition site of I_{ORCa} also does not involve a channel-associated kinase domain (discussed in Matsushita et al., 2005).

Here we show that several polyvalent cations, such as polyamines, trivalent metals, neomycin, and polylysine, as well as ammonium inhibit endogenous MIC and expressed TRPM7 currents (Fig. 1). This lack of specificity suggests that the Mg^{2+}-binding site is unlikely to be within a defined site of the protein itself, as bulky molecules like poly-L-lysine would not be expected to fit into a metal binding site. Since these same cations also inhibited IRK1, a well-known $PI(4,5)P_2$- dependent channel (Huang et al., 1998), we reasoned that they most probably act in a similar manner on the MIC channel by screening the negatively charged head groups of $PI(4,5)P_2$. The polyamine potency of MIC current inhibition depends strongly on the charge, supporting this hypothesis.

Physiological Regulation of MIC/TRPM7 Channel Activity

Our results demonstrate that raising internal pH is sufficient to activate MIC current during whole-cell or perforated-patch recording. In the latter configuration, divalent cations (and consequently Mg^{2+}) inside the cell are not dialyzed and remain at physiological levels. Yet extracellular NH_4^+ can overcome the inhibition of MIC current by these cations. Addition of a weak base to the external solution activated MIC current, and weak acids inhibited it. The site of action is internal, since effects of weak bases or acids were significantly attenuated by increased internal pH buffer capacity and were mimicked by dialysis of acidic internal solutions both delivered from the pipette solution (Fig. 6). TRPM7 current was greatly diminished during cell-attached recording by addition of acetate to the bath, an effect consistent with a diffusible messenger (protons) since the pipette solution did not contain acetate. Our data

suggest that internal protons inhibit I_{MIC} in the same way that Mg^{2+} does: by screening $PI(4,5)P_2$ head group charges (Bell, 1986; Toner et al., 1988). Until now, the only known way to activate MIC channels was prolonged whole-cell dialysis with a solution lacking Mg^{2+} (Hermosura et al., 2002; Kozak et al., 2002; Jiang et al., 2003). Therefore, TRPM7 joins the group of other TRP family channels in having a possible sensory mode of activation (Gunthorpe et al., 2002; Vennekens et al., 2002). Most interestingly, TRPM7 senses the pH of the interior of the cell, whereas the majority of sensory TRP channels detect external stimuli. The current findings demonstrate that depletion of Mg^{2+} is not the only stimulus for I_{MIC} activation; it is very possible that washout of cellular spermine and reduction in H^+ concentration serve as additional (and additive) stimuli. Indeed, the local concentration of charged inhibitors may be higher at membrane surface, due to acidic lipids that regulate the channel activity. Perfusion of Mg^{2+}-free recording solutions supplemented with commonly used strong pH buffers, such as HEPES, may effectively raise the pH near the plasma membrane in parallel with reduction of Mg^{2+}. The contribution of spermine to the tonic inhibition of I_{MIC} in native tissues such as T lymphocytes is less likely since the free spermine concentration in mammalian cells is estimated at <100 μM (Aidley and Stanfield, 1996), an order of magnitude below its effective inhibitory concentration. We cannot rule out the possibility that local spermine concentrations near the channel are higher than the bulk values and may be sufficient to exert significant inhibition.

PIP$_2$ Screening and Channel Rundown

Ion channel rundown has been documented extensively in patch-clamp experiments (Byerly and Yazejian, 1986; Kozlowski and Ashford, 1990; Horn and Korn, 1992). The underlying reason for the gradual and irreversible loss of channel activity during prolonged whole-cell recording is thought to be the loss of factors necessary for channel function, since rundown generally does not occur during perforated-patch recording. Rundown can depend upon posttranslational changes of the channel protein due to altered phosphorylation (McDonald et al., 1994), washout of an interacting protein component (Xu et al., 2004), or changes in lipid–protein interactions (Huang et al., 1998; Zhang et al., 1999). We believe that inward rectifier K^+ channels and MIC/TRPM7 channels share the latter type of mechanism. IRK channel rundown is dependent on micromolar Mg^{2+} concentrations and can be prevented by addition of the Mg^{2+} chelator EDTA (Kozlowski and Ashford, 1990), as we show here for MIC/TRPM7 (Fig. 5). Huang et al. (1998) were first to demonstrate that IRK channel rundown can be reversed by phosphoinosi-

tides applied to the inner surface of the plasma membrane (see Fig. 10 for comparison on MIC/TRPM7). It is thought that rundown results from PIP$_2$ depletion caused by Mg^{2+}-dependent lipid phosphatases or phospholipases (Hilgemann and Ball, 1996; Zhang et al., 1999). We observed that rundown of both MIC and IRK1 was completely prevented by internally applied EDTA/HEDTA to remove residual internal Mg^{2+} that would normally produce rundown (Figs. 5, 9, and 11). The difference in time course of MIC and IRK current rundown (Fig. 3) and differences in the number of preactivated channels could indicate a lower affinity for PIP$_2$ (Huang et al., 1998) or a lower effective concentration near the MIC channel. Cations that inhibit I_{MIC} at millimolar concentrations are likely to cause its rundown at micromolar concentrations. Accordingly, we found that Mg^{2+} (at micromolar concentrations) was not unique at promoting rundown. Neomycin, a well-known PLC inhibitor (Schacht, 1976; Prentki et al., 1986), had a similar effect in the absence of Mg^{2+} (Fig. 5 D). This effect is therefore unlikely to reflect activation of lipid phospholipases.

Our explanation for MIC channel rundown differs from the accepted one for inward rectifier K^+ channels that is based upon experiments in which recovery of channel function is affected by adding PIP$_2$ in inside-out patches (Huang et al., 1998; Zhang et al., 1999; Zeng et al., 2002). We hypothesize that PIP$_2$ is required to open the channel and that positively charged cations (Mg^{2+}, polyamines, and protons) in cytosol can screen or bind to phosphates on PIP$_2$ and reduce the effective concentration of the negatively charged lipid species near the channel. Since PIP$_2$ levels are initially high, MIC current is activated when Mg^{2+} is reduced. After prolonged recording, however, when PIP$_2$ levels have fallen, a physiological pH is sufficient to prevent current activation because protons bind to PIP$_2$ (Toner et al., 1988). Thus, when the local PIP$_2$ concentration is reduced, the channel–PIP$_2$ interactions become more susceptible to screening by protons (at pH 7.3) and micromolar Mg^{2+} concentrations, leading to rundown. This inhibition can be relieved by NH_4^+ acting to increase local pH during whole-cell or perforated patch recording or by alkaline pH applied directly in inside-out patches (Figs. 5, 7, and 9). In all three cases, MIC channel activity was increased. Native I_{MIC} rundown during whole-cell recording can be reversed completely by NH_4^+-induced cytosolic alkalinization (Fig. 5 C). Increasing pH directly in inside-out patches, but without increasing PIP$_2$ concentration, also reversed rundown of the recombinant TRPM7 channels (Fig. 11). At longer times as PIP$_2$ is reduced further, I_{MIC} runs down even in the presence of external NH_4^+ (unpublished data), suggesting that alkaline pH does not modify the behavior of the channels drastically, but

only increases the effective PIP_2 concentration that promotes channel opening. Our model for inhibition and rundown predicts that the effects of different cations would be additive. This prediction was confirmed by experiments with varying internal Mg^{2+} concentrations and applying external NH_4^+ (Fig. 4). Mg^{2+} at a given concentration was effective only when enough protons were present (physiological pH); at more alkaline pH this same concentration of Mg^{2+} was no longer sufficient to inhibit the current. If internal Mg^{2+} concentration was elevated ($\sim$8–10 mM), NH_4^+ no longer activated the current, presumably because high concentrations of Mg^{2+} are sufficient to screen all PIP_2 charges even when there are fewer protons.

In these studies, we demonstrate that extracellular NH_4^+ application can be used for recovery of channels from rundown during prolonged recording. Sensitivity to extracellular NH_4^+ will be a potentially useful test for PIP_2 depletion-mediated rundown. Future efforts should be directed at identifying the protein sites that interact with PIP_2. Basic amino acid residues are known to interact with phosphoinositide head groups in other proteins such as gelsolin (Yu et al., 1992), inwardly rectifying K^+ channels (Huang et al., 1998; Ho and Murrell-Lagnado, 1999; Zhang et al., 1999; Shyng et al., 2000; Rohacs et al., 2003; Suh and Hille, 2005) and other proteins (for review see McLaughlin et al., 2002). Several TRP channels have been shown to be PIP2 sensitive (Chuang et al., 2001; Estacion et al., 2001; Runnels et al., 2002; for review see Hardie, 2003). It is likely that TRPM7 domains interacting with phosphoinositides will also contain positively charged amino acids.

REFERENCES

Aidley, D.J., and P.R. Stanfield. 1996. Ion channels. Cambridge University Press, Cambridge. 307 pp.

Alvarez, O., M. Brodwick, R. Latorre, A. McLaughlin, S. McLaughlin, and G. Szabo. 1983. Large divalent cations and electrostatic potentials adjacent to membranes. Experimental results with hexamethonium. *Biophys. J.* 44:333–342.

Antonenko, Y.N., P. Pohl, and G.A. Denisov. 1997. Permeation of ammonia across bilayer lipid membranes studied by ammonium ion selective microelectrodes. *Biophys. J.* 72:2187–2195.

Bell, J. 1986. The sarcoplasmic reticulum potassium channel. Lipid effects. *In* Ion Channel Reconstitution. Plenum Press, New York. 469–482.

Boldt, M., G. Burckhardt, and B.C. Burckhardt. 2003. NH_4^+ conductance in *Xenopus laevis* oocytes. III. Effect of NH_3. *Pflugers Arch.* 446:652–657.

Boron, W.F. 1983. Transport of H^+ and of ionic weak acids and bases. *J. Membr. Biol.* 72:1–16.

Boron, W.F. 1986. Intracellular pH regulation in epithelial cells. *Annu. Rev. Physiol.* 48:377–388.

Boron, W.F., A. Roos, and P. De Weer. 1978. NH_4Cl and other weak bases in the activation of sea urchin eggs. *Nature.* 274:190.

Byerly, L., and B. Yazejian. 1986. Intracellular factors for the maintenance of calcium currents in perfused neurones from the snail, *Lymnaea stagnalis. J. Physiol.* 370:631–650.

Chalfie, M., Y. Tu, G. Euskirchen, W.W. Ward, and D.C. Prasher. 1994. Green fluorescent protein as a marker for gene expression. *Science.* 263:802–805.

Cherny, V.V., L.M. Henderson, and T.E. DeCoursey. 1997. Proton and chloride currents in Chinese hamster ovary cells. *Membr. Cell Biol.* 11:337–347.

Chuang, H.H., E.D. Prescott, H. Kong, S. Shields, S.E. Jordt, A.I. Basbaum, M.V. Chao, and D. Julius. 2001. Bradykinin and nerve growth factor release the capsaicin receptor from PtdIns(4,5)P2-mediated inhibition. *Nature.* 411:957–962.

Clapham, D.E. 2002. Sorting out MIC, TRP, and CRAC ion channels. *J. Gen. Physiol.* 120:217–220.

Clapham, D.E. 2003. TRP channels as cellular sensors. *Nature.* 426:517–524.

Estacion, M., W.G. Sinkins, and W.P. Schilling. 2001. Regulation of *Drosophila* transient receptor potential-like (TrpL) channels by phospholipase C-dependent mechanisms. *J. Physiol.* 530:1–19.

Estevez, A.Y., R.K. Roberts, and K. Strange. 2003. Identification of store-independent and store-operated Ca^{2+} conductances in *Caenorhabditis elegans* intestinal epithelial cells. *J. Gen. Physiol.* 122:207–223.

Fakler, B., U. Brandle, E. Glowatzki, S. Weidemann, H.P. Zenner, and J.P. Ruppersberg. 1995. Strong voltage-dependent inward rectification of inward rectifier K^+ channels is caused by intracellular spermine. *Cell.* 80:149–154.

Fan, Z., and J.C. Makielski. 1997. Anionic phospholipids activate ATP-sensitive potassium channels. *J. Biol. Chem.* 272:5388–5395.

Gabev, E., J. Kasianowicz, T. Abbott, and S. McLaughlin. 1989. Binding of neomycin to phosphatidylinositol 4,5-bisphosphate (PIP_2). *Biochim. Biophys. Acta.* 979:105–112.

Golowasch, J., A. Kirkwood, and C. Miller. 1986. Allosteric effects of Mg^{2+} on the gating of Ca^{2+}-activated K^+ channels from mammalian skeletal muscle. *J. Exp. Biol.* 124:5–13.

Gomperts, B.D., I.M. Kramer, and P.E. Tatham. 2003. Signal Transduction. Elsevier Academic Press, Amsterdam. 420 pp.

Grubbs, R.D. 2002. Intracellular magnesium and magnesium buffering. *Biometals.* 15:251–259.

Gunthorpe, M.J., C.D. Benham, A. Randall, and J.B. Davis. 2002. The diversity in the vanilloid (TRPV) receptor family of ion channels. *Trends Pharmacol. Sci.* 23:183–191.

Guo, D., and Z. Lu. 2000. Mechanism of IRK1 channel block by intracellular polyamines. *J. Gen. Physiol.* 115:799–814.

Gwanyanya, A., B. Amuzescu, S.I. Zakharov, R. Macianskiene, K.R. Sipido, V.M. Bolotina, J. Vereecke, and K. Mubagwa. 2004. Magnesium-inhibited, TRPM6/7-like channel in cardiac myocytes: permeation of divalent cations and pH-mediated regulation. *J. Physiol.* 559:761–776.

Hanks, S.K., and T. Hunter. 1995. Protein kinases 6. The eukaryotic protein kinase superfamily: kinase (catalytic) domain structure and classification. *FASEB J.* 9:576–596.

Hardie, R.C. 2003. Regulation of TRP channels via lipid second messengers. *Annu. Rev. Physiol.* 65:735–759.

Hermosura, M.C., M.K. Monteilh-Zoller, A.M. Scharenberg, R. Penner, and A. Fleig. 2002. Dissociation of the store-operated calcium current I_{CRAC} and the Mg-nucleotide-regulated metal ion

current MagNuM. *J. Physiol.* 539:445–458.

Hilgemann, D.W., and R. Ball. 1996. Regulation of cardiac Na$^+$,Ca^{2+} exchange and KATP potassium channels by PIP$_2$. *Science*. 273:956–959.

Ho, I.H., and R.D. Murrell-Lagnado. 1999. Molecular mechanism for sodium-dependent activation of G protein-gated K$^+$ channels. *J. Physiol.* 520:645–651.

Horn, R., and S.J. Korn. 1992. Prevention of rundown in electrophysiological recording. *Methods Enzymol.* 207:149–155.

Huang, C.L., S. Feng, and D.W. Hilgemann. 1998. Direct activation of inward rectifier potassium channels by PIP$_2$ and its stabilization by Gβγ. *Nature*. 391:803–806.

Jiang, X., E.W. Newell, and L.C. Schlichter. 2003. Regulation of a TRPM7-like current in rat brain microglia. *J. Biol. Chem.* 278:42867–42876.

Kerschbaum, H.H., J.A. Kozak, and M.D. Cahalan. 2003. Polyvalent cations as permeant probes of MIC and TRPM7 pores. *Biophys. J.* 84:2293–2305.

Kozak, J.A., and M.D. Cahalan. 2003. MIC channels are inhibited by internal divalent cations but not ATP. *Biophys. J.* 84:922–927.

Kozak, J.A., and M.D. Cahalan. 2004. Regulation of MIC and TRPM7 channels by internal polyvalent cations. *Biophys.* J. 86:663 (Abstr.).

Kozak, J.A., S. Misler, and D.E. Logothetis. 1998. Characterization of a Ca^{2+}-activated K$^+$ current in insulin-secreting murine βTC-3 cells. *J. Physiol.* 509:355–370.

Kozak, J.A., H.H. Kerschbaum, and M.D. Cahalan. 2002. Distinct properties of CRAC and MIC channels in RBL cells. *J. Gen. Physiol.* 120:221–235.

Kozak, J.A., M. Matsushita, A.C. Nairn, and M.D. Cahalan. 2005. TRPM7 current is activated by intracellular alkalinization. *Biophys. J.* 88:2291 (Abstr.).

Kozlowski, R.Z., and M.L. Ashford. 1990. ATP-sensitive K$^+$-channel run-down is Mg^{2+} dependent. *Proc. R. Soc. Lond. B. Biol. Sci.* 240:397–410.

Langner, M., and K. Kubica. 1999. The electrostatics of lipid surfaces. *Chem. Phys. Lipids.* 101:3–35.

Lopatin, A.N., E.N. Makhina, and C.G. Nichols. 1994. Potassium channel block by cytoplasmic polyamines as the mechanism of intrinsic rectification. *Nature*. 372:366–369.

Manning, G., G.D. Plowman, T. Hunter, and S. Sudarsanam. 2002a. Evolution of protein kinase signaling from yeast to man. *Trends Biochem. Sci.* 27:514–520.

Manning, G., D.B. Whyte, R. Martinez, T. Hunter, and S. Sudarsanam. 2002b. The protein kinase complement of the human genome. *Science.* 298:1912–1934.

Matsushita, M., J.A. Kozak, Y. Shimizu, D.T. McLachlin, H. Yamaguchi, F.Y. Wei, K. Tomizawa, H. Matsui, B.T. Chait, M.D. Cahalan, and A.C. Nairn. 2005. Channel function is dissociated from the intrinsic kinase activity and autophosphorylation of TRPM7/ChaK1. *J. Biol. Chem.* 280:20793–20803.

McDonald, T.F., S. Pelzer, W. Trautwein, and D.J. Pelzer. 1994. Regulation and modulation of calcium channels in cardiac, skeletal, and smooth muscle cells. *Physiol. Rev.* 74:365–507.

McLaughlin, S. 1989. The electrostatic properties of membranes. *Annu. Rev. Biophys. Biophys. Chem.* 18:113–136.

McLaughlin, S., N. Mulrine, T. Gresalfi, G. Vaio, and A. McLaughlin. 1981. Adsorption of divalent cations to bilayer membranes containing phosphatidylserine. *J. Gen. Physiol.* 77:445–473.

McLaughlin, S., J. Wang, A. Gambhir, and D. Murray. 2002. PIP$_2$ and proteins: interactions, organization, and information flow. *Annu. Rev. Biophys. Biomol. Struct.* 31:151–175.

Minke, B., and B. Cook. 2002. TRP channel proteins and signal transduction. *Physiol. Rev.* 82:429–472.

Montell, C. 2003. Mg^{2+} Homeostasis: The Mg^{2+}nificent TRPM Chanzymes. *Curr. Biol.* 13:R799–R801.

Montell, C., L. Birnbaumer, and V. Flockerzi. 2002. The TRP channels, a remarkably functional family. *Cell.* 108:595–598.

Nadler, M.J., M.C. Hermosura, K. Inabe, A.L. Perraud, Q. Zhu, A.J. Stokes, T. Kurosaki, J.P. Kinet, R. Penner, A.M. Scharenberg, and A. Fleig. 2001. LTRPC7 is a Mg.ATP-regulated divalent cation channel required for cell viability. *Nature*. 411:590–595.

Ng, L.L., J.E. Davies, and M.C. Garrido. 1991. Intracellular free magnesium in human lymphocytes and the response to lectins. *Clin. Sci. (Lond.).* 80:539–547.

Prakriya, M., and R.S. Lewis. 2002. Separation and characterization of currents through store-operated CRAC channels and Mg^{2+}-inhibited cation (MIC) channels. *J. Gen. Physiol.* 119:487–507.

Prentki, M., J.T. Deeney, F.M. Matschinsky, and S.K. Joseph. 1986. Neomycin: a specific drug to study the inositol-phospholipid signalling system? *FEBS Lett.* 197:285–288.

Rae, J., K. Cooper, P. Gates, and M. Watsky. 1991. Low access resistance perforated patch recordings using amphotericin B. *J. Neurosci. Methods.* 37:15–26.

Rohacs, T., C.M. Lopes, T. Jin, P.P. Ramdya, Z. Molnar, and D.E. Logothetis. 2003. Specificity of activation by phosphoinositides determines lipid regulation of Kir channels. *Proc. Natl. Acad. Sci. USA.* 100:745–750.

Roos, A., and W.F. Boron. 1981. Intracellular pH. *Physiol. Rev.* 61:296–434.

Runnels, L.W., L. Yue, and D.E. Clapham. 2002. The TRPM7 channel is inactivated by PIP$_2$ hydrolysis. *Nat. Cell Biol.* 4:329–336.

Ryazanova, L.V., M.V. Dorovkov, A. Ansari, and A.G. Ryazanov. 2004. Characterization of the protein kinase activity of TRPM7/ChaK1, a protein kinase fused to the transient receptor potential ion channel. *J. Biol. Chem.* 279:3708–3716.

Schacht, J. 1976. Inhibition by neomycin of polyphosphoinositide turnover in subcellular fractions of guinea-pig cerebral cortex in vitro. *J. Neurochem.* 27:1119–1124.

Schmitz, C., A.L. Perraud, C.O. Johnson, K. Inabe, M.K. Smith, R. Penner, T. Kurosaki, A. Fleig, and A.M. Scharenberg. 2003. Regulation of vertebrate cellular Mg^{2+} homeostasis by TRPM7. *Cell.* 114:191–200.

Shi, J., and J. Cui. 2001. Intracellular Mg^{2+} enhances the function of BK-type Ca^{2+}-activated K$^+$ channels. *J. Gen. Physiol.* 118:589–606.

Shyng, S.L., and C.G. Nichols. 1998. Membrane phospholipid control of nucleotide sensitivity of KATP channels. *Science.* 282:1138–1141.

Shyng, S.L., C.A. Cukras, J. Harwood, and C.G. Nichols. 2000. Structural determinants of PIP$_2$ regulation of inward rectifier K(ATP) channels. *J. Gen. Physiol.* 116:599–608.

Siraganian, R.P., A. McGivney, E.L. Barsumian, F.T. Crews, F. Hirata, and J. Axelrod. 1982. Variants of the rat basophilic leukemia cell line for the study of histamine release. *Fed. Proc.* 41:30–34.

Stewart, A.K., M.N. Chernova, B.E. Shmukler, S. Wilhelm, and S.L. Alper. 2002. Regulation of AE2-mediated Cl$^-$ transport by intracellular or by extracellular pH requires highly conserved amino acid residues of the AE2 NH$_2$-terminal cytoplasmic domain. *J. Gen. Physiol.* 120:707–722.

Strong, J.A., and S.A. Scott. 1992. Divalent-selective voltage-independent calcium channels in *Lymnaea* neurons: permeation properties and inhibition by intracellular magnesium. *J. Neurosci.* 12:2993–3003.

Suh, B.C., and B. Hille. 2005. Regulation of ion channels by phosphatidylinositol 4,5-bisphosphate. *Curr. Opin. Neurobiol.* 15:370–378.

Takezawa, R., C. Schmitz, P. Demeuse, A.M. Scharenberg, R. Penner, and A. Fleig. 2004. Receptor-mediated regulation of the

TRPM7 channel through its endogenous protein kinase domain. *Proc. Natl. Acad. Sci. USA*. 101:6009–6014.

Toner, M., G. Vaio, A. McLaughlin, and S. McLaughlin. 1988. Adsorption of cations to phosphatidylinositol 4,5-bisphosphate. *Biochemistry*. 27:7435–7443.

Vennekens, R., T. Voets, R.J. Bindels, G. Droogmans, and B. Nilius. 2002. Current understanding of mammalian TRP homologues. *Cell Calcium*. 31:253–264.

Xu, J.J., L.Y. Hao, A. Kameyama, and M. Kameyama. 2004. Calmodulin reverses rundown of L-type Ca^{2+} channels in guinea pig ventricular myocytes. *Am. J. Physiol. Cell Physiol*. 287:C1717–C1724.

Yamaguchi, H., M. Matsushita, A.C. Nairn, and J. Kuriyan. 2001. Crystal structure of the atypical protein kinase domain of a TRP channel with phosphotransferase activity. *Mol. Cell*. 7:1047–1057.

Yazejian, B., and L. Byerly. 1989. Voltage-independent barium-permeable channel activated in *Lymnaea* neurons by internal perfusion or patch excision. *J. Membr. Biol*. 107:63–75.

Yu, F.X., H.Q. Sun, P.A. Janmey, and H.L. Yin. 1992. Identification of a polyphosphoinositide-binding sequence in an actin monomer-binding domain of gelsolin. *J. Biol. Chem*. 267:14616–14621.

Zeng, W.Z., H.H. Liou, U.M. Krishna, J.R. Falck, and C.L. Huang. 2002. Structural determinants and specificities for ROMK1-phosphoinositide interaction. *Am. J. Physiol. Renal Physiol*. 282:F826–F834.

Zhang, H., C. He, X. Yan, T. Mirshahi, and D.E. Logothetis. 1999. Activation of inwardly rectifying K^+ channels by distinct PtdIns(4,5)P_2 interactions. *Nat. Cell Biol*. 1:183–188.